
Unified Long-Term Time-Series Forecasting Benchmark

Jacek Cyranka
Institute of Informatics
University of Warsaw
Poland
jcyranka@gmail.com

Szymon Haponiuk
Institute of Informatics
University of Warsaw
Poland

Abstract

In order to support the advancement of machine learning methods for predicting time-series data, we present a comprehensive dataset designed explicitly for long-term time-series forecasting. We incorporate a collection of datasets obtained from diverse, dynamic systems and real-life records. Each dataset is standardized by dividing it into training and test trajectories with predetermined lookback lengths. We include trajectories of length up to 2000 to ensure a reliable evaluation of long-term forecasting capabilities. To determine the most effective model in diverse scenarios, we conduct an extensive benchmarking analysis using classical and state-of-the-art models, namely LSTM, DeepAR, NLinear, N-Hits, PatchTST, and LatentODE. Our findings reveal intriguing performance comparisons among these models, highlighting the dataset-dependent nature of model effectiveness. Notably, we introduce a custom latent NLinear model and enhance DeepAR with a curriculum learning phase. Both consistently outperform their vanilla counterparts.

1 Introduction

Time-series (TS) forecasting is a fundamental task in contemporary data analysis, aiming to predict future events based on historical data. Its broad applicability across various domains, including strategic planning, resource allocation, risk management, and control design, underscores its importance. Consequently, extensive research efforts have been dedicated to developing efficient and accurate long-term time-series forecasting (LTSF) methods within the machine learning (ML) and applied statistics communities. The ideal LTSF method should provide an end-to-end solution capable of handling diverse time-series data characteristics across domains. However, determining the optimal default method for a specific LTSF task and ensuring reliable out-of-the-box performance remains a challenge. The landscape of available methods encompasses deep learning-based approaches, continuous time models, statistical techniques, and more. Each method class has its advantages and an active research community. Notably, deep neural network (NN) models have recently experienced rapid advancements in the context of the LTSF problem [Lim and Zohren, 2021, Torres et al., 2021, Lara-Benítez et al., 2021], motivating our focus on evaluating such models within our benchmark. In LTSF research, the availability of large and diverse datasets is crucial for training and benchmarking contemporary ML models. While natural language processing benefits from abundant data, time-series datasets still lag behind in quantity and diversity. For example, training foundational models for time-series analysis necessitates access to substantial and varied data. As highlighted by Zhou et al. [2023], the largest existing dataset for time-series analysis falls below 10GB, whereas our dataset exceeds 100 GB.

Existing LTSF datasets can be broadly classified into two categories. First, real-life datasets are sourced from diverse domains, such as temperature records, traffic data, and weather observations. However, these datasets often suffer from being univariate or treated dimension by dimension, limiting their suitability for comprehensive evaluation. Second, researchers resort to custom synthetic

datasets, including benchmarks like the long-range arena [Tay et al., 2021] for TS classification or data generated from chaotic dynamical systems [Gilpin, 2021]. Nevertheless, relying solely on restricted scenario datasets hampers fair performance comparisons across state-of-the-art methods and impedes determining the best overall approach. Furthermore, NN trained by supervised learning is susceptible to overfitting, which may also be the case in time-series forecasting, and some models may excel on specific benchmarks while struggling to generalize across different domains.

We introduce a unified LTSF benchmark dataset encompassing data from diverse domains to address the abovementioned limitations. We curate instances from established real-life datasets while leveraging synthetic data generation techniques to construct clean trajectories of arbitrary length without missing values. By providing this unified dataset, we aim to enable fair and comprehensive evaluations of LTSF methods, promoting a deeper understanding of their strengths and weaknesses across various domains. In practical applications of time-series forecasting, methods capable of producing predictions valid over extended periods are highly desirable. This allows for weather forecasts spanning weeks, long-term stock market trend predictions, or robot behaviors for model predictive control designs.

Presently, it is common practice to evaluate LTSF approaches using extended forecasted sequence lengths, reaching up to 720-time steps. However, we observe a lack of standardization regarding the length of the lookback window used as input for forecasting models. Notably, the selection of the lookback window is often fine-tuned for a specific model. For example, linear models are typically trained with long, fixed lookbacks, while transformer-based models employ shorter, variable-length histories. In this work, we propose a unified TS forecasting benchmark that addresses the identified gaps in existing benchmarks.

1. Dataset Diversity: We recognized dataset diversity’s importance in comprehensively evaluating LTSF methods. To address this gap, we curated datasets from various domains, including robotic simulations with stochastic and deterministic control, partial differential equations, deterministic chaotic dynamics, and real-life data. By incorporating datasets from diverse domains, we aim to provide a more representative benchmark for LTSF.

2. Facilitating Training and Testing ML Models: We split the datasets into training and testing trajectories to ensure standardized evaluations and comparisons. Each separate trajectory has a fixed length, typically set to 1000 time steps and up to 2000. This approach allows for consistent and reproducible evaluations across different methods. Additionally, we explicitly provide the desired history window lengths for each dataset, which provides a notion of various difficulty levels, e.g., shorter lookbacks make the forecasting task more challenging; on the other hand, longer lookbacks make encoding of the history more challenging. We emphasize that for the synthetic datasets, opposite to real-life datasets, each trajectory is separate and different, i.e., there is no overlap; hence, different lookback lengths, in fact, define different problems, and by doing so, we test the expressivity of the studied approaches.

3. Introduction of New Hand-Crafted Models: We recognized the need to explore and evaluate new models not tested before in the context of LTSF. Our research introduces two models: the latent NLinear model and DeepAR enhanced with curriculum learning (CL). These models have not been previously applied to LTSF tasks, and their inclusion in the benchmark is intended to highlight their performance and potential. We observed significant improvements across the entire dataset when using these models, suggesting their effectiveness as baselines for LTSF.

Having the unified dataset, we perform a thorough benchmark of a suite of NN-based methods, including classical approaches like LSTM, DeepAR, and latent ordinary differential equation (ODE) with recently published newer approaches demonstrated to improve the forecasting accuracy over the existing methods: SpaceTime, N-Hits, LTSF NLinear, and Patch transformer. Last but not least, we share an open-source library with state-of-the-art implementations as a toolkit in the PyTorch framework to help accelerate progress in the field.

1.1 Related Work

The most dominant class of LTSF benchmarks relies on datasets with rather uniform characteristics composed of nine widely-used real-world datasets: Electricity Transformer Temperature (ETT) from Zhou et al. [2021a] (split into four cases: ETTh1, ETTh2, ETTm1, ETTm2), Traffic, Electricity, Weather, ILI, ExchangeRate. All of them are univariate time series with a significant degree of non-

deterministic (these are real-life measurements). Our introduced unified LTSF benchmark dataset consists of a few distinct classes of LTSF datasets mixing uni/multi-variate and real-life/synthetic. On the other hand, the long-range arena benchmark by Tay et al. [2021] introduces synthetic binary images used as a time-series classification challenge. In the NLP domain, synthetically generated data are increasingly used for training models capable of basic reasoning at smaller scales [Gunasekar et al., 2023, Li et al., 2023, Eldan and Li, 2023]. In this work, we introduce a few synthetic TS datasets and focus exclusively on the forecasting task. A separate set of benchmarks with irregularly sampled time-stamps exist but is not suitable for long-term forecasting, the challenge being in irregular sample modeling: Electronic Health Records (Physionet) the data set of the Physionet Computing in Cardiology Challenge 2012 [Silva et al., 2012] and Climate Data (USHCN) The United States Historical Climatology Network (USHCN) dataset. The Physionet dataset contains data of 8000 ICU patients and 72 different time points per patient on average. Monash Time Series Forecasting Archive [Godahewa et al., 2021] compiles a set of 30 univariate real-life datasets from various domains. It evaluates statistical approaches for LTSF, Bauer et al. [2021] introduces a larger univariate real-life time-series collection. In this work, we benchmark NN-based approaches using diverse TS datasets: uni/multi-variate and real-life/synthetic. Another collection of uniform characteristics chaotic datasets dedicated for TS forecasting by Gilpin [2021] benchmark various ML models in this uniform setting. The UCR time series archive is dedicated to time-series classification task [Dau et al., 2019]. Refer to Tab. 1 for a summary of related benchmark datasets. It is visible that our compressed dataset is significantly larger than the other available TS benchmark datasets; we choose the compressed size metric for comparison, as it reflects trajectory overlaps; in particular, real-life datasets are more amenable for compression than synthetic ones. For instance, 20k synthetic trajectories with up to 2k timestamped states result in 40M distinct states in total.

Table 1: Comparison of our benchmark dataset to prior work.

Benchmark	compressed size	origin	domain	forecasting	classification	eval. methods
ETT [Zhou et al., 2021a]	4Mb	real-life	electric	yes	no	transformers
LLA [Tay et al., 2021]	7 700Mb	synthetic	planar paths	no	yes	transformers
Monash [Godahewa et al., 2021]	501Mb	real-life	diverse	yes	no	statistical
Libra [Bauer et al., 2021]	542Mb	real-life	diverse	yes	no	statistical & ML
Chaos [Gilpin, 2021]	80Mb	synthetic	chaos	yes	no	statistical & NN
UCR [Dau et al., 2019]	316Mb	real-life	diverse	no	yes	N/A
ours	100 000Mb	real-life & synthetic	diverse	yes	no	NN

2 Datasets

We introduce all of the datasets included in our benchmark. Some of the datasets are scattered in various earlier works on LTSF. However, our work is the first that unifies several diverse domains within a single self-contained benchmark dataset. A summary of the synthetic datasets in our benchmark is in Tab. 2. We share unnormalized datasets in hdf5 raw format online dat. All datasets are split into training and test/evaluation sets. Data is normalized using the standard normalization with std. dev. and mean values computed over the whole training set, then test data are normalized with the pre-computed values. All synthetic datasets contain 20k trajectories, from which the first 18k are used for training and 2k are dedicated for evaluation/testing. We emphasize that the trajectories in synthetic datasets do not overlap, i.e., each is generated using a different initial condition. We provide only a training dataset and a test dataset. However, in a typical data-science workflow, it would be recommended to use the validation set as well. We only have a distinct test dataset for simplicity, but one could also split the training dataset into a training and validation set. The synthetic datasets include 2k test trajectories, which leaves space for splitting this set into validation/test.

2.1 Synthetic

Sinewave. The deterministic univariate sinewave series comprises quasi-periodic trajectories defined by $s_j = \sin(0.2 \cdot j + \phi) + \sin(0.3 \cdot j + \phi)$, where ϕ is a random phase $\phi \in [0, 1]$, drawn from the uniform distribution per trajectory basis. We generate trajectories by setting j to a sequence of integers. We include the dataset generated by a simple deterministic periodic rule as an instance of a sanity check in our benchmark suite. The obtained results are surprisingly varied. Some methods rapidly converge to numerical zero, whereas others, including DeepAR and LSTM, fail to converge.

Mackey-Glass. Mackey-Glass (MG) is a family of univariate Delayed differential equation (DDE) modeling certain biological behavior [Mackey and Glass, 1977]. For some range of parameters, the equation admits chaotic attractors. The equations take the form $\frac{dy}{dt} = \frac{0.2y(t-\tau)}{1+y^{10}(t-\tau)} - 0.1y(t)$, where τ is the delay which we fix to $\tau = 25$, the equation demonstrates chaotic dynamics for this particular τ value. We generate the trajectories by applying the Euler scheme with time-step 0.1 to the delayed dynamical system with uniformly random initial history per trajectory – 10τ points sampled from the range $1.2 + [-0.01, 0.01]$. The main difficulty of the MG dataset lies in modeling the chaotic dynamics exhibiting high sensitivity to the initial history; the forecasting problem is especially challenging for shorter context windows.

Lorenz. Lorenz dynamical system is a simplified meteorological model shown to admit a chaotic attractor (the Lorenz butterfly), i.e., all trajectories are contained within a compact butterfly-shaped region but exhibit very high sensitivity to the initial condition (IC). We use the classical parameters $\sigma = 10, \rho = 28, \beta = 8/3$; the trajectories are generated by following a random IC sampled from the normal distribution centered at $(0, -0.01, 9)$ with std. dev. 0.001 using the Euler scheme with time-step 0.01. The dataset is multivariate (three variables), and the main difficulty of the Lorenz dataset lies in modeling the chaotic dynamics exhibiting high sensitivity to the initial history; the forecasting problem is especially challenging for shorter context windows.

Stochastic Lotka-Volterra. The deterministic Lotka-Volterra (LV) dynamical system models the predator-prey population dynamics. It is a system of coupled nonlinear ordinary differential equations (ODEs): $\frac{dx}{dt} = \alpha x - \beta xy, \frac{dy}{dt} = \delta xy - \gamma y$, with x, y denoting the prey and predator populations respectively. We set the parameters: the growth rate of prey population $\alpha = 1$, the effect of the presence of predators on the prey growth rate $\beta = 0.1$, the effect of the presence of prey on the predator’s growth rate $\delta = 0.02$, the predator’s death rate $\gamma = 0.5$. The initial condition is sampled uniformly per each trajectory from the range $(50, 150), (10, 30)$. Stochasticity is injected at each step by uniformly sampling $\alpha \in [1 - 0.002, 1 + 0.002]$. The deterministic LV exhibits stable periodic dynamics, but the added stochasticity perturbs the dynamics, resulting in random fluctuations, and a forecasting method aims to predict the rough trend of the population dynamics.

Kuramoto-Sivashinsky. We find it instructive to evaluate the models on a smooth chaotic dynamical system with a large spatial dimension (100). We chose the 1d Kuramoto-Sivashinsky (KS) fourth-order nonlinear partial differential equation (PDE) exhibiting chaotic dynamics: $u_t + u_{xx} + u_{xxxx} + \frac{1}{2}u_x^2 = 0$ with periodic boundary conditions on the interval domain $[0, 200]$. Solution u is the flame velocity. Following the setup given in Linot and Graham [2022] we generated trajectories of length 1000 initiating from a random initial condition – weighted sum of $\sin(y)$ & $\cos(y)$, where $y \in \{x\pi/32, x\pi/16, x\pi/8, x\pi/4\}$ with uniform random weights. We used the spectral method with 100 coefficients for solving the PDE in the frequency space, applying the fast Fourier transform (FFT) and time-stepping using the Runge-Kutta (RK) scheme with $dt = 0.01$. Each trajectory is rolled out until time $t = 200$, and trajectories of length 1000 are generated, saving one in 20 frames. There are two main difficulties of the forecasting task for the KS dataset: the equation is chaotic and exhibits high sensitivity to the initial condition; the spatial dimension is large (100), requiring an efficient state encoding in a forecasting method.

Cahn-Hilliard. Apart from chaotic dynamics, an abundance of stable physical processes is amenable to forecasting given short input sequences; such data may be of a significant spatial dimension. We choose the Cahn-Hilliard (CH) PDE often encountered in research on pattern formation. The dynamics of the equation for a given parameter value and the initial condition are stable and lead to the formation of one of the stable patterns. We solve the CH equation $\partial c/\partial t = \nabla^2(c^3 - c - 0.0001 \cdot \nabla^2 c)$ in a 2D domain $\Omega = [0, 1]^2$ with periodic boundary conditions. Solution c is the concentration of the fluid $c \in [-1, 1]$. The equation is solved in the frequency space using the spectral method (applying the FFT) using 64×64 grid, and the RK scheme does the time-stepping with $dt = 5e - 06$. The dataset trajectories are generated by saving each frame and recording the 16×16 uniform subgrid of each frame. The dataset consists of stable trajectories having a vast state dimension (256), requiring efficient state encoding in a forecasting method.

MuJoCo. We generated six datasets using the MuJoCo [Todorov et al., 2012] rigid body dynamics simulator. MuJoCo is a widely used benchmark environment in the reinforcement learning domain, where model-based approaches are based on learning a forecasting model from data for an efficient controller design. Hence, it is crucial to demonstrate guidelines for picking the suitable forecasting model in such an environment. Data is generated using three environments (Half-Cheetah, Walker2d,

and Hopper). We use the D4RL framework from Fu et al. [2020]. Using the pretrained policies for each task, we generate 18k training and 2k test trajectories of total length 1000. We apply the so-called medium policies from the D4RL suite that are trained up to 1/3 of the maximal return reached by the Soft Actor-Critic (SAC) RL algorithm (an expert policy). We are ensuring that the trajectories in the dataset are diverse. Two modes of control possible using stochastic policies obtained by SAC: the deterministic actions (D) and the actions sampled randomly from the policy normal distribution (S). We obtain two datasets per environment by following the two different control modes. The MuJoCo datasets consist of trajectories exhibiting complex dynamics with a significant state dimension 11-17, obtained through an external controller.

Table 2: Synthetic datasets. All datasets contain 20k trajectories in total.

PROBLEM	DOMAIN	TRAJ. LENGTH	OBS. DIM.	LOOKBACKS	DETERM.
SINEWAVE OSCILLATOR	SIMPLE SIGNAL (SANITY CHECK)	2000	1	2,8,96	✓
STOCHASTIC LOTKA-VOLTERRA	SDE, POPULATION DYN.	2000	2	96, 500, 2000	✗
MACKEY-GLASS	DDE, CHAOS	2000	1	96,500,1000	✓
LORENZ	ODE, CHAOS	2000	3	96,500,1000	✓
MUJoCo HOPPER D	RL, ROBOTIC SIM.	1000	11	96, 250, 500	✓
MUJoCo CHEETAH D	RL, ROBOTIC SIM.	1000	17	96, 250, 500	✓
MUJoCo WALKER2D D	RL, ROBOTIC SIM.	1000	17	96, 250, 500	✓
MUJoCo HOPPER S	RL, ROBOTIC SIM.	1000	11	96, 250, 500	✗
MUJoCo CHEETAH S	RL, ROBOTIC SIM.	1000	17	96, 250, 500	✗
MUJoCo WALKER2D S	RL, ROBOTIC SIM.	1000	17	96, 250, 500	✗
KURAMOTO-SIVASHINSKY PDE	PDE, CHAOS	1000	100	96, 250, 500	✓
CAHN-HILLARD PDE	PDE, STABLE PATTERN FORMATION	1000	256	96, 250, 500	✓

Table 3: Real-life datasets.

PROBLEM	DOMAIN	TOTAL # TRAJS.	TRAJ. LENGTH	OBS. DIM.	LOOKBACKS
M4	FINANCE	289094	247	1	96, 168
ETTM 1 + 2	ELECTRICITY	133602	1440	1	96, 336, 720
ELECTRICITY	ELECTRICITY	1083452	1440	1	96, 336, 720
ETTM 1 + 2 (LONG)	ELECTRICITY	131362	2000	1	1000
WEATHER	WEATHER	208295	1000	21	96, 250, 500
PEMS-BAY	TRAFFIC	51542	288	325	144

2.2 Real-life

The summary of real-life datasets included in our benchmark is in Tab. 3. We emphasize that the trajectories in real-life datasets are generated using overlapping, i.e., a long trajectory is split into several overlapping sub-trajectories.

M4. We took weekly time series from the M4 competition dataset [Makridakis et al., 2020], a financial data with exact origin not revealed. We preprocessed the raw data. We filtered out these series shorter than 247 (It gave us a good balance between the number of series and their length). We have used the first 240 trajectories as the training dataset and the rest as the test dataset (variable length). For every trajectory in the original dataset, we included all 247-length overlapping sub-trajectories in the respective final dataset (train/test). We do not include the newer M5 dataset. Upon closer inspection, we found that M5 would be more suited towards a hand-crafted forecasting procedure (inc., hierarchical forecasting and specific feature engineering). We found a subset of M4 more suitable for our effort.

ETTM 1 + 2. We have used two series from the ETT-small dataset (m1 and m2) introduced by Zhou et al. [2021b]. The data is recorded from electrical transformers gathered in two regions of China in 15-minute intervals. First, We have divided them into the training and test datasets (initial 80% going into the training dataset). The series was then divided into lengths 1440 in the same fashion as in the M4 dataset. Moreover, we use a long variant with trajectories of length 2000. There are seven variables in the dataset. The most popular option is forecasting one target variable (the remaining six are exogenous). *Electricity*. We have used the 370 series from the Household Electric Power Consumption data [ele]. They were divided the same way as the M4 dataset (trajectories of length 1440, with training/test datasets split on at 2014-08-31 23:00). For computational reasons. We used a random 1/8 of the resulting trajectories for training and testing.

Weather. We have used the daily records of weather data (21 measurements) shared in *wea*. We merged the data from years 2019 to 2022 inclusive into one trajectory and divided it into overlapping subtrajectories of length 1000.

PEMS-BAY. Traffic dataset collected by California Transportation Agencies (CalTrans) Performance Measurement System (PEMS) used in Li et al. [2018]. Selected 325 sensors in the Bay Area (BAY), collected during 6 first months of 2017. The dataset has the largest state dimension of all of the included datasets.

2.3 Benchmark Synergy

Our dataset comprises two main components: real-life datasets commonly used in the recent literature, the PEMS-BAY traffic dataset, contrary to the standard datasets, characterized by a large number of interacting channels, and a collection of clean, diverse synthetic datasets on top of that. These datasets serve as a reference point and provide a foundation for benchmarking the performance of LTSF ML models. Complementing the real-life datasets, we have included a set of synthetic datasets that pose different challenges. Tab. 2 shows that our synthetic collection complements the real-life datasets in several aspects (lengths, obs. dim., degree of stochasticity). We leverage the flexibility of a broad spectrum of synthetic datasets to exhibit significantly longer trajectories, with up to 2k steps, and possess larger spatial dimensions, reaching up to 256 in the case of the Cahn-Hillard PDE. Furthermore, the synthetic datasets encompass simulated dynamical systems, such as the rigid body dynamics of robots using MuJoCo, which is particularly relevant for control design. We incorporate two modes of control, deterministic and stochastic, to account for different control strategies. Moreover, the systems belong into two distinct categories: those exhibiting regular stable dynamics (e.g., Lotka-Volterra with stochasticity, Cahn-Hillard PDE) and those exhibiting chaotic dynamics (e.g., Mackey-Glass, Lorenz, Kuramoto-Sivashinsky PDE). By combining real-life and synthetic datasets, we believe our benchmark dataset provides a comprehensive evaluation framework to assess the performance of NN and, in general, ML models in time-series forecasting. We hope some datasets will be included in further ML model benchmarks. Including diverse scenarios enables a more robust analysis and facilitates the exploration of model generalization across different applications. The prescribed lookback lengths are adjusted per dataset basis and were chosen based on the setting studied in previous work, i.e., short, medium, and long lookback lengths are set, where the longest lookback length is set to the first half of the total trajectory length, and the shortest is less than 10% of the total trajectory length.

3 Benchmarked Machine Learning Models

We briefly present the state-of-the-art NN-based models that we benchmarked. We have focused on the classical approach to time series. We do not include spatio-temporal graph models, which work well with datasets such as PEMS-BAY, but this was the only dataset we used with a clear graph representation. All of the custom implementation improvements are provided. We share a self-contained PyTorch library comprising the standardized implementations of all the models (except the PatchTST, for which we used the original repository) cod. Tables with the used hyperparameters can be found in the appendix. In most cases, we relied on the original hyperparameters provided by the authors, in some cases requiring slight tuning. PDE problems and the longest forecasting horizons are infeasible for some models (excluded from Tab. 4).

LSTM [Hochreiter and Schmidhuber, 1997]. The long-short term memory (LSTM) model is a special kind of recurrent neural network capable of learning long-term dependencies in data. LSTM models time series using the latent space (whose dimension is a hyperparameter). It is trained in the sequence-to-sequence fashion. We include LSTM as a baseline, demonstrating strong performance for some datasets.

DeepAR [Salinas et al., 2020]. DeepAR is an LSTM-based recurrent neural network trained in the autoregressive fashion contrary to the vanilla LSTM model. The original algorithm is trained to output a probability distribution, which may be used as, e.g., uncertainty estimates. However, we used a modified DeepAR implementation outputting point estimates. Apart from that, we train the model backpropagating through the whole horizon, automatically using a prediction from timestep t as input for timestep $t + 1$.

DeepAR + CL (ours). We implement our customized DeepAR model enhanced with a curriculum learning phase. We adapt the widely known curriculum learning technique [Graves et al., 2017, Cirik et al., 2016] for TS forecasting. Before the actual model training on the full-length trajectories, a ‘warm-start’ phase is first performed in which the encoder and the model are pretrained on shorter trajectories of gradually increasing lengths. We demonstrate that such modified training consistently improves the performance of the vanilla DeepAR.

Latent ODE [Rubanova et al., 2019]. Neural ODEs [Chen et al., 2018] is one of the most influential families of continuous recurrent neural network models. Neural ODEs define a time-dependent hidden state $h(t)$ as the solution to the initial value problem $\frac{dh(t)}{dt} = f_\theta(h(t), t)$, $h(t_0) = t_0$ and f_θ is a NN parametrized by a vector θ . We used a nongenerative setting, a smaller architecture than the original work, with an LSTM encoder and an multi-layer perceptron (MLP) decoder. Nonetheless, the LTSF setting is still challenging for NODE models due to the sequential nature of ODE solvers. For real-life datasets, we have used the same curriculum learning technique as for DeepAR, which also significantly improved its performance. We are training the model in a standard non-VAE fashion.

N-Hits [Challu et al., 2022]. An improvement of the earlier model N-Beats by Oreshkin et al. [2020]. Incorporating hierarchical interpolation and multi-rate data sampling techniques, N-HITS sequentially assembles predictions while emphasizing different frequency components and scales. This approach effectively decomposes the input signal and synthesizes forecasts. We have modified the original implementation to add support for multivariate time series.

LTSF NLinear [Zeng et al., 2023]. As described by the authors, an ‘embarrassingly simple one-layer linear model’ was demonstrated to outperform the sophisticated transformer-based models in real-life datasets. LTSF Linear models are trained in sequence-to-sequence fashion and operate directly on the states; hence, they are challenging to apply for datasets with larger dimensional states. One modification that we have applied is working on the flattened states, i.e. model is not channel independent and thus is very parameter heavy for high-dimensional data.

Latent LTSF NLinear (ours). In order to circumvent the limitations of LTSF Linear models about restricted state-space dimension and modeling of nonlinear dependencies between the state components, we introduce the latent LTSF NLinear model. The linear map is applied to the latent representations of states instead of the states directly. Our model outperforms the vanilla LTSF NLinear in most benchmarked datasets and can be applied to problems with large spatial dimensions (PDEs). We used an LSTM encoder and an MLP decoder. To limit the parameter count, the latent dimension is set to be smaller than the observation space for a high-dimensional series.

SpaceTime [Zhang et al., 2023]. A recent State-space model (SSM) is dedicated to effective time-series modeling. SSMs are classical models for time series, and prior works combine SSMs with deep learning layers for efficient sequence modeling (S4 and subsequent models). It can express complex dependencies, forecast over long horizons, and efficiently train over long sequences. Contrary to the S4 model, it can model autoregressive processes.

Patch Transformer [Nie et al., 2023] (PatchTST). At the time of submission, this is the newest model from the LTSF transformer family, shown to outperform the earlier transformer models for time-series forecasting and the LTSF-Linear[Zeng et al., 2023]. PatchTST employs self-supervised representation learning. It is based on segmenting time series into subseries-level patches, which serve as input tokens. We have modified the original implementation to allow for a direct interaction between series variables.

4 Benchmark Results

We present the thorough NN model benchmark results on the introduced dataset. Space considerations defer some of our experimental results to the appendix. In all subsequent tables, minimal mean-squared error (MSE) and mean absolute error (MAE) metrics were reported achieved during training on the test set (2k trajectories). The best results are marked with boldface and blue color. We report results truncated to two decimal places. We share spreadsheets with precise results online cod.

We now describe how the LTSF task is set up. Given $L < N$ *lookback window* size (also called the history). Let $X = (s_0, s_1, \dots, s_{L-1})$, $Y = (s_L, \dots, s_N)$ be a trajectory not seen during the training phase split into the initial chunk of length L (the lookback window length) and the remainder of length $T = N - L$ (the future). The task of a forecasting model is to predict \hat{Y} given X such that

$\|\hat{Y} - Y\|$ is minimized, where $\|\cdot\|$ is either the usual MSE or MAE metric. We set the lookback windows based on the setting studied in previous work, i.e., short, medium, and long lookback lengths are used, where the longest lookback length is set to the first half of the total trajectory length, and the shortest is less than 10% of the total trajectory length.

Benchmark results of methods presented in Sec. 4 on the synthetic datasets from Sec. 2.1 are presented in Tab. 4. Benchmark results of methods presented in Sec. 4 on the synthetic datasets from Sec. 2.2 are presented in Tab. 5.

4.1 Computational Methodology

Each of the experiments was performed on an RTX2080Ti GPU card or equivalent. Each experiment was run until convergence by visual investigation of the loss curves or until reaching the global 8 hours cap. We utilized a modest computational cluster in an academic setting comprised of 16 GPUs. The whole benchmark required performing 335 runs, giving 2680 GPU hours in total. The rate of performing optimization epochs and hence the convergence rate is highly model specific. We can, nonetheless, provide some insights into the convergence speeds of different methods. Usually, the fastest to converge are N-Hits, NLinear, and LSTM, which typically will converge well below the specified hard limit. Other methods (DeepAR, PatchTST, NeuralODE, SpaceTime) may take a time close to the limit to converge. The lowest to converge is Neural ODE, due to the sequential solver employed for rolling out trajectories. If the model for given parameters did not fit on a single GPU, we attempted to fit it by decreasing its size (layer widths etc.). If the metric values are not reported for the given model in Sec. 4, it means that it was infeasible to perform such an evaluation. To account for varied convergence speeds, we set a global runtime cap uniform for all datasets equal to 8 hours.

5 Benchmark Conclusions

We present our paper’s key findings, which we believe hold significant implications for the machine learning community and offer valuable insights for future developments in research on NN models dedicated to LTSF. See Fig. 1 for bar plots visualizing the benchmark results averaged over classes.

Need of sanity check datasets. As demonstrated by our sanity-check dataset – the Sinewave (results in Tab. 4), surprisingly, such a simple dataset diversifies the NN models. Not all of the models performing well in more complicated scenarios managed to converge here on much simpler signal data. In particular, LSTM and DeepAR models stand out and struggle to converge even in the case of the larger lookback (96). We note that CL alleviates the issue to some extent. PatchTST diverges for short lookbacks (1, 2) but still converges for larger.

Best models depend on the dataset. The notion that newer models always outperform older ones is challenged by our findings. While the newer models (N-Hits, NLinear, SpaceTime, PatchTST) dominate the older LSTM and DeepAR approaches in real-life data (see Tab.5), the situation changes dramatically with synthetic datasets. The performance rankings are shuffled, highlighting the importance of considering the dataset characteristics. When focusing on low-dimensional, long-trajectory datasets (as shown in Tab.4), LSTM performs the best, with N-Hits proving competitive for chaotic datasets, thus confirming observations made in previous studies [Gilpin, 2021]. In the case of the previously unexplored MuJoCo data, classical LSTM and DeepAR (with CL) models exhibit the best performance. Training the models not shown for the PDE datasets (refer to Tab. 4) is infeasible. The best performer depends on the equation, with DeepAR + CL excelling in the chaotic KS Case and PatchTST prevail in the stable but high-dimensional CH case. We noted that we had altered its original implementation to allow for inter-variable communication, and the original implementation might not perform as well.

Underappreciated baselines: Classical NN models. We emphasize that the classical approaches, LSTM and DeepAR, have often been overlooked as baselines. However, our experiments reveal their consistently strong performance compared to state-of-the-art models. Therefore, we argue that these models deserve to be included in the evaluated baselines, particularly when addressing LTSF scenarios beyond the standard set of univariate real-life datasets.

DeepAR + CL and Latent LTSF models are competitive. We emphasize that DeepAR + CL and Latent LTSF models beat their vanilla counterparts in almost the entire benchmark. CL opens the possibility of applying DeepAR in the LTSF setting, and the Latent NLinear variant opens the possibility of

Table 4: Benchmark Results on the synthetic datasets described in Sec. 2.1. The resulting metrics are shown rounded to two decimal places. The numbers shown in the first table were also multiplied by 100.

DATASET	L	N-HITS		SPACE TIME		LATENT NLINEAR		NLINEAR		DEEPAR CL		LSTM		DEEPAR VANILLA		NEURAL ODE		PATCHT	
		MSE	MAE	MSE	MAE	MSE	MAE	MSE	MAE	MSE	MAE	MSE	MAE	MSE	MAE	MSE	MAE	MSE	MAE
SIN.	1	0.0	0.0	0.0	0.8	0.1	1.8	33.2	44.1	69.0	70.1	87.5	71.2	98.3	79.9	98.8	80.3	607.1	188.2
	2	0.0	0.0	0.0	0.6	0.0	0.2	1.8	10.2	53.6	63.4	79.9	66.7	98.9	80.2	98.9	80.3	1071.7	253.1
	8	0.0	0.0	0.0	0.4	0.0	0.0	0.0	0.0	3.0	13.3	85.2	70.1	99.0	80.4	99.7	81.0	0.0	1.2
	96	0.0	0.0	0.0	0.9	0.0	0.0	0.0	0.0	3.7	14.9	77.0	63.1	99.6	81.0	100.5	81.4	0.1	1.5
AVG.		0.0	0.0	0.0	0.7	0.0	0.5	8.7	13.6	32.3	40.4	82.4	67.8	98.9	80.4	99.5	80.7	419.7	111.0

DATASET	L	LSTM		N-HITS		LATENT NLINEAR		DEEPAR CL		SPACE TIME		NEURAL ODE		NLINEAR		DEEPAR VANILLA		PATCHT	
		MSE	MAE	MSE	MAE	MSE	MAE	MSE	MAE	MSE	MAE	MSE	MAE	MSE	MAE	MSE	MAE	MSE	MAE
L.-V.	96	0.80	0.61	0.83	0.63	0.81	0.61	0.81	0.62	0.83	0.63	0.90	0.68	0.89	0.68	0.89	0.67	0.99	0.69
	500	0.78	0.59	0.80	0.61	0.79	0.59	0.79	0.59	0.81	0.63	0.87	0.66	0.84	0.64	0.87	0.65	0.95	0.66
	1000	0.63	0.49	0.71	0.55	0.70	0.53	0.64	0.50	0.87	0.67	0.78	0.60	0.87	0.67	0.76	0.58	0.82	0.58
M.-G.	96	0.67	0.59	0.64	0.55	0.68	0.58	0.80	0.69	0.74	0.64	0.96	0.79	0.82	0.70	1.00	0.82	0.77	0.64
	500	0.66	0.58	0.74	0.63	0.80	0.67	0.70	0.62	0.81	0.71	0.88	0.76	0.90	0.76	0.98	0.81	0.88	0.73
	1000	0.49	0.46	0.73	0.64	0.78	0.66	0.96	0.60	0.99	0.82	0.86	0.75	0.92	0.77	0.96	0.80	0.86	0.72
LORENZ	96	0.56	0.51	0.48	0.43	0.54	0.49	0.61	0.55	0.63	0.57	0.76	0.67	0.69	0.60	0.66	0.59	0.70	0.55
	500	0.60	0.54	0.58	0.52	0.61	0.53	0.67	0.60	0.76	0.68	0.84	0.74	0.84	0.73	0.90	0.78	0.94	0.74
	1000	0.47	0.43	0.67	0.59	0.71	0.62	0.83	0.63	0.97	0.82	0.80	0.70	0.88	0.75	0.65	0.60	1.05	0.81
AVG.		0.63	0.53	0.69	0.57	0.71	0.59	0.76	0.60	0.82	0.69	0.85	0.71	0.85	0.70	0.85	0.70	0.88	0.68

DATASET	L	DEEPAR CL		LSTM		SPACE TIME		LATENT NLINEAR		N-HITS		NLINEAR		DEEPAR VANILLA		NEURAL ODE		PATCHT	
		MSE	MAE	MSE	MAE	MSE	MAE	MSE	MAE	MSE	MAE	MSE	MAE	MSE	MAE	MSE	MAE	MSE	MAE
CHEETAH	96	0.79	0.71	0.80	0.72	0.80	0.72	0.80	0.72	0.82	0.73	0.81	0.73	0.90	0.79	0.91	0.80	0.91	0.77
	250	0.76	0.69	0.77	0.70	0.78	0.71	0.78	0.71	0.82	0.73	0.80	0.72	0.95	0.82	0.95	0.82	0.89	0.75
	500	0.68	0.64	0.68	0.65	0.70	0.66	0.70	0.66	0.77	0.69	0.73	0.68	0.94	0.82	0.89	0.79	0.80	0.70
HOPPER	96	0.72	0.48	0.72	0.48	0.73	0.49	0.73	0.48	0.74	0.49	0.75	0.51	0.72	0.48	0.74	0.50	1.14	0.63
	250	0.75	0.48	0.74	0.48	0.77	0.50	0.77	0.50	0.79	0.52	0.81	0.53	0.75	0.48	0.79	0.52	1.16	0.64
	500	0.63	0.44	0.63	0.44	0.67	0.47	0.68	0.48	0.69	0.50	0.73	0.52	0.65	0.45	0.68	0.48	0.95	0.58
WALKER	96	0.86	0.65	0.86	0.64	0.87	0.65	0.87	0.65	0.88	0.65	0.88	0.66	0.87	0.65	0.87	0.66	1.28	0.79
	250	0.85	0.62	0.85	0.62	0.87	0.64	0.89	0.65	0.91	0.67	0.94	0.70	0.85	0.62	0.90	0.66	1.30	0.80
	500	0.68	0.50	0.69	0.50	0.76	0.57	0.75	0.56	0.80	0.59	0.83	0.63	0.69	0.50	0.73	0.54	1.06	0.69
AVG.		0.75	0.58	0.75	0.58	0.77	0.60	0.77	0.60	0.80	0.62	0.81	0.63	0.81	0.62	0.83	0.64	1.06	0.71

DATASET	L	PATCHT		SPACE TIME		DEEPAR CL		LSTM		LATENT NLINEAR		DEEPAR VANILLA	
		MSE	MAE	MSE	MAE	MSE	MAE	MSE	MAE	MSE	MAE	MSE	MAE
K.-S.	96	1.05	0.85	0.97	0.81	0.92	0.78	0.96	0.81	0.99	0.82	0.96	0.81
	250	1.06	0.85	0.97	0.82	0.90	0.77	0.97	0.81	1.00	0.83	0.97	0.81
	500	1.04	0.84	0.97	0.82	0.86	0.74	0.94	0.79	0.99	0.82	0.93	0.79
C.-H.	96	0.46	0.52	0.57	0.63	1.01	0.89	0.74	0.71	0.83	0.78	1.00	0.88
	250	0.36	0.45	0.49	0.58	0.59	0.64	0.73	0.71	0.87	0.79	1.00	0.86
	500	0.27	0.39	0.79	0.74	0.50	0.57	0.67	0.66	0.89	0.80	1.17	0.97
AVG.		0.71	0.65	0.79	0.73	0.80	0.73	0.84	0.75	0.93	0.81	1.01	0.85

applying Linear models in problems with high space dimensions. To the best of our knowledge, our work is the first to evaluate and demonstrate the high performance of these models across various LTSF scenarios, offering strong competition to the recently introduced state-of-the-art approaches.

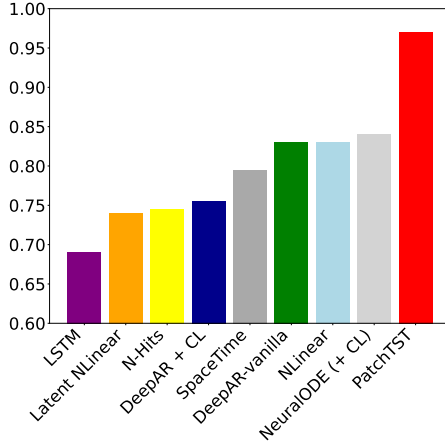
6 Future Work and Conclusions

We proposed a new LTSF benchmark dataset and extensive benchmark of the current state-of-the-art. We are convinced that our contribution holds implications for the machine learning community and offers valuable insights for future developments in research on the ML approach to LTSF. Each benchmarked model involves its own set of hyperparameters, and it was out of this work's scope to fine-tune them carefully. Performed benchmark provides first insights on the performance of the

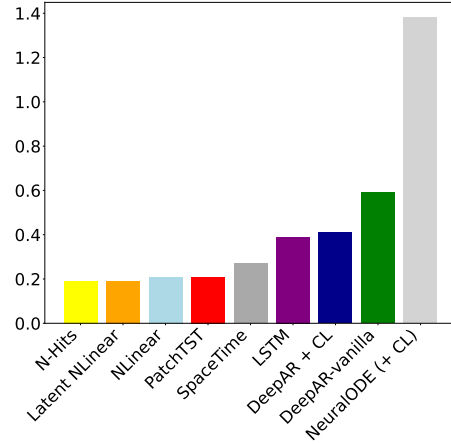
Table 5: Benchmark Results on the real-life datasets described in Sec. 2.2. The resulting metrics are shown rounded to two decimal places.

DATASET	L	N-HITS		LATENT NLINEAR		NLINEAR		PATCHT		SPACE TIME		LSTM		DEEPAR CL		DEEPAR VANILLA		NEURAL ODE	
		MSE	MAE	MSE	MAE	MSE	MAE	MSE	MAE	MSE	MAE	MSE	MAE	MSE	MAE	MSE	MAE	MSE	MAE
ETTM1+2	96	0.21	0.33	0.22	0.33	0.23	0.35	0.22	0.34	0.21	0.33	0.24	0.35	0.23	0.34	0.35	0.44	0.32	0.41
	336	0.17	0.30	0.18	0.30	0.19	0.32	0.17	0.31	0.17	0.31	0.21	0.33	0.18	0.32	0.22	0.34	0.33	0.44
	720	0.15	0.29	0.15	0.28	0.16	0.29	0.15	0.29	0.17	0.31	0.17	0.30	0.18	0.31	0.19	0.32	0.96	0.78
M4	96	0.21	0.22	0.22	0.22	0.25	0.25	0.21	0.21	0.20	0.22	0.22	0.23	0.24	0.23	0.24	0.24	0.24	0.25
	168	0.12	0.16	0.14	0.16	0.14	0.17	0.13	0.15	0.12	0.16	0.14	0.16	0.13	0.17	0.13	0.16	0.15	0.19
ELECTRIC	96	0.30	0.05	0.29	0.05	0.35	0.05	0.36	0.06	0.15	0.05	0.91	0.10	0.99	0.10	1.52	0.17	4.55	1.58
	336	0.21	0.05	0.19	0.04	0.26	0.05	0.32	0.05	0.13	0.05	0.72	0.10	0.85	0.10	1.26	0.21	4.73	1.28
	720	0.17	0.04	0.19	0.04	0.11	0.03	0.19	0.04	0.25	0.07	0.70	0.09	0.71	0.10	1.13	0.18	0.82	0.12
ETTM (LONG)	1000	0.17	0.30	0.16	0.29	0.16	0.30	0.16	0.30	1.02	0.92	0.19	0.32	0.19	0.32	0.32	0.43	0.30	0.41
AVG.		0.19	0.19	0.19	0.19	0.21	0.20	0.21	0.20	0.27	0.27	0.39	0.22	0.41	0.22	0.59	0.28	1.38	0.61

DATASET	L	LATENT NLINEAR		LSTM		SPACE TIME		DEEPAR CL		DEEPAR VANILLA		PATCHT		N-HITS		NLINEAR	
		MSE	MAE	MSE	MAE	MSE	MAE	MSE	MAE	MSE	MAE	MSE	MAE	MSE	MAE	MSE	MAE
PEMS-BAY	144	0.68	0.41	0.67	0.36	0.69	0.39	0.71	0.38	0.73	0.38	N/A	N/A	N/A	N/A	N/A	N/A
WEATHER	96	0.71	0.43	0.72	0.43	0.73	0.45	0.75	0.45	0.88	0.54	0.91	0.46	0.82	0.47	0.98	0.49
	250	0.69	0.42	0.69	0.42	0.71	0.43	0.75	0.45	0.87	0.54	0.81	0.43	0.85	0.46	0.86	0.47
	500	0.66	0.41	0.67	0.41	0.69	0.43	0.72	0.43	0.73	0.44	0.72	0.40	0.83	0.45	0.76	0.45
AVG.		0.68	0.42	0.69	0.41	0.71	0.42	0.73	0.43	0.80	0.47	0.81	0.43	0.83	0.46	0.86	0.47



(a) MSE averaged over chaotic and MuJoCo datasets



(b) MSE averaged over univariate real-life datasets

Figure 1: Barplots illustrating the relative performance of the benchmarked methods over synthetic and real-life datasets (taking into account those feasible by the entirety of methods only). Note Fig. 1a is rescaled.

models for default or close to default hyper-parameters and the method robustness to hyperparameter values. Further fine-tuning the models for better performance in diverse scenarios is an important future research direction.

7 Acknowledgements

The project is financed by the Polish National Agency for Academic Exchange. Both authors have been partly supported by the NAWA Polish Returns grant PPN/PPO/2018/1/00029. JC have been supported by IDUB UW grant Nowe Idee. This research was supported in part by PL-Grid Infrastructure.

References

- Long-horizon forecasting benchmark code. https://drive.google.com/drive/folders/1S16bDiihE6xARB1uMN1AeWq5ByCqkTMI?usp=drive_link. Accessed: 2023-09-27.
- Long-horizon forecasting benchmark datasets. https://drive.google.com/drive/folders/1fAHpka3hu2kM4j6ebzAPnGpLpSMnTlf?usp=drive_link. Accessed: 2023-09-27.
- Uci machine learning repository: Electricityloaddiagrams20112014 data set. URL <https://archive.ics.uci.edu/ml/datasets/ElectricityLoadDiagrams20112014>. Accessed: 2023-06-02.
- Weather station on top of the roof of the institute building of the max-planck-institute for biogeochemistry. URL https://www.bgc-jena.mpg.de/wetter/weather_data.html.
- André Bauer, Marwin Züfle, Simon Eismann, Johannes Grohmann, Nikolas Herbst, and Samuel Kounev. Libra: A benchmark for time series forecasting methods. In *Proceedings of the ACM/SPEC International Conference on Performance Engineering, ICPE '21*, page 189–200, New York, NY, USA, 2021. Association for Computing Machinery. ISBN 9781450381949. doi: 10.1145/3427921.3450241. URL <https://doi.org/10.1145/3427921.3450241>.
- Cristian Challu, Kin G. Olivares, Boris N. Oreshkin, Federico Garza, Max Mergenthaler-Canseco, and Artur Dubrawski. N-hits: Neural hierarchical interpolation for time series forecasting, 2022.
- Tian Qi Chen, Yulia Rubanova, Jesse Bettencourt, and David K. Duvenaud. Neural ordinary differential equations. In *NeurIPS*, pages 6572–6583, 2018. URL <http://papers.nips.cc/paper/7892-neural-ordinary-differential-equations>.
- Tianqi Chen and Carlos Guestrin. Xgboost: A scalable tree boosting system. *CoRR*, abs/1603.02754, 2016. URL <http://arxiv.org/abs/1603.02754>.
- Volkan Cirik, Eduard H. Hovy, and Louis-Philippe Morency. Visualizing and understanding curriculum learning for long short-term memory networks. *ArXiv*, abs/1611.06204, 2016.
- Hoang Anh Dau, Anthony Bagnall, Kaveh Kamgar, Chin-Chia Michael Yeh, Yan Zhu, Shaghayegh Gharghabi, Chotirat Ann Ratanamahatana, and Eamonn Keogh. The ucr time series archive. *IEEE/CAA Journal of Automatica Sinica*, 6(6):1293–1305, 2019. doi: 10.1109/JAS.2019.1911747.
- Ronen Eldan and Yuanzhi Li. Tinstories: How small can language models be and still speak coherent english?, 2023.
- Justin Fu, Aviral Kumar, Ofir Nachum, George Tucker, and Sergey Levine. D4rl: Datasets for deep data-driven reinforcement learning, 2020.
- William Gilpin. Chaos as an interpretable benchmark for forecasting and data-driven modelling. In *Thirty-fifth Conference on Neural Information Processing Systems Datasets and Benchmarks Track (Round 2)*, 2021. URL <https://openreview.net/forum?id=enYjtbjYJrf>.
- Rakshitha Wathsadini Godahewa, Christoph Bergmeir, Geoffrey I. Webb, Rob Hyndman, and Pablo Montero-Manso. Monash time series forecasting archive. In *Thirty-fifth Conference on Neural Information Processing Systems Datasets and Benchmarks Track (Round 2)*, 2021. URL <https://openreview.net/forum?id=wEc1mgAjU->.
- Alex Graves, Marc G. Bellemare, Jacob Menick, Rémi Munos, and Koray Kavukcuoglu. Automated curriculum learning for neural networks. In *Proceedings of the 34th International Conference on Machine Learning - Volume 70, ICML'17*, page 1311–1320. JMLR.org, 2017.
- Suriya Gunasekar, Yi Zhang, Jyoti Aneja, Caio César Teodoro Mendes, Allie Del Giorno, Sivakanth Gopi, Mojan Javaheripi, Piero Kauffmann, Gustavo de Rosa, Olli Saarikivi, Adil Salim, Shital Shah, Harkirat Singh Behl, Xin Wang, Sébastien Bubeck, Ronen Eldan, Adam Tauman Kalai, Yin Tat Lee, and Yuanzhi Li. Textbooks are all you need, 2023.
- Sepp Hochreiter and Jürgen Schmidhuber. Long short-term memory. *Neural computation*, 9:1735–80, 12 1997. doi: 10.1162/neco.1997.9.8.1735.
- Pedro Lara-Benítez, Manuel Carranza-García, and José C. Riquelme. An experimental review on deep learning architectures for time series forecasting. *International Journal of Neural Systems*, 31(03):2130001, 2021. doi: 10.1142/S0129065721300011. URL <https://doi.org/10.1142/S0129065721300011>. PMID: 33588711.

- Yaguang Li, Rose Yu, Cyrus Shahabi, and Yan Liu. Diffusion convolutional recurrent neural network: Data-driven traffic forecasting. In *International Conference on Learning Representations (ICLR '18)*, 2018.
- Yuanzhi Li, Sébastien Bubeck, Ronen Eldan, Allie Del Giorno, Suriya Gunasekar, and Yin Tat Lee. Textbooks are all you need ii: phi-1.5 technical report, 2023.
- Bryan Lim and Stefan Zohren. Time-series forecasting with deep learning: a survey. *Philosophical transactions. Series A, Mathematical, physical, and engineering sciences*, 379:20200209, 04 2021. doi: 10.1098/rsta.2020.0209.
- Alec J. Linot and Michael D. Graham. Data-driven reduced-order modeling of spatiotemporal chaos with neural ordinary differential equations. *Chaos: An Interdisciplinary Journal of Nonlinear Science*, 32(7):073110, 2022. doi: 10.1063/5.0069536. URL <https://doi.org/10.1063/5.0069536>.
- Michael C. Mackey and Leon Glass. Oscillation and chaos in physiological control systems. *Science*, 197 4300: 287–9, 1977.
- Spyros Makridakis, Evangelos Spiliotis, and Vassilios Assimakopoulos. The m4 competition: 100,000 time series and 61 forecasting methods. *International Journal of Forecasting*, 36(1):54–74, 2020. ISSN 0169-2070. doi: <https://doi.org/10.1016/j.ijforecast.2019.04.014>. URL <https://www.sciencedirect.com/science/article/pii/S0169207019301128>. M4 Competition.
- Yuqi Nie, Nam H Nguyen, Phanwadee Sinthong, and Jayant Kalagnanam. A time series is worth 64 words: Long-term forecasting with transformers. In *The Eleventh International Conference on Learning Representations*, 2023. URL <https://openreview.net/forum?id=Jbdc0vT0col>.
- Boris N. Oreshkin, Dmitri Carpov, Nicolas Chapados, and Yoshua Bengio. N-beats: Neural basis expansion analysis for interpretable time series forecasting. In *International Conference on Learning Representations*, 2020. URL <https://openreview.net/forum?id=r1ecqn4YwB>.
- Yulia Rubanova, Ricky T. Q. Chen, and David K Duvenaud. Latent ordinary differential equations for irregularly-sampled time series. In H. Wallach, H. Larochelle, A. Beygelzimer, F. d'Alché-Buc, E. Fox, and R. Garnett, editors, *Advances in Neural Information Processing Systems*, volume 32. Curran Associates, Inc., 2019. URL <https://proceedings.neurips.cc/paper/2019/file/42a6845a557bef704ad8ac9cb4461d43-Paper.pdf>.
- David Salinas, Valentin Flunkert, Jan Gasthaus, and Tim Januschowski. Deepar: Probabilistic forecasting with autoregressive recurrent networks. *International Journal of Forecasting*, 36(3):1181–1191, 2020. ISSN 0169-2070. doi: <https://doi.org/10.1016/j.ijforecast.2019.07.001>. URL <https://www.sciencedirect.com/science/article/pii/S0169207019301888>.
- Ikaro Silva, George B. Moody, Daniel J. Scott, Leo Anthony Celi, and Roger G. Mark. Predicting in-hospital mortality of icu patients: The physionet/computing in cardiology challenge 2012. *2012 Computing in Cardiology*, pages 245–248, 2012.
- Yi Tay, Mostafa Dehghani, Samira Abnar, Yikang Shen, Dara Bahri, Philip Pham, Jinfeng Rao, Liu Yang, Sebastian Ruder, and Donald Metzler. Long range arena : A benchmark for efficient transformers. In *International Conference on Learning Representations*, 2021. URL <https://openreview.net/forum?id=qVyeW-grC2k>.
- Emanuel Todorov, Tom Erez, and Yuval Tassa. Mujoco: A physics engine for model-based control. In *IROS*, pages 5026–5033. IEEE, 2012. ISBN 978-1-4673-1737-5. URL <http://dblp.uni-trier.de/db/conf/iros/iros2012.html#TodorovET12>.
- José F. Torres, Dalil Hadjout, Abderrazak Sebaa, Francisco Martínez-Álvarez, and Alicia Troncoso. Deep learning for time series forecasting: A survey. *Big Data*, 9(1):3–21, 2021. doi: 10.1089/big.2020.0159. URL <https://doi.org/10.1089/big.2020.0159>. PMID: 33275484.
- Ailing Zeng, Muxi Chen, Lei Zhang, and Qiang Xu. Are transformers effective for time series forecasting? 2023.
- Michael Zhang, Khaled Kamal Saab, Michael Poli, Tri Dao, Karan Goel, and Christopher Re. Effectively modeling time series with simple discrete state spaces. In *The Eleventh International Conference on Learning Representations*, 2023. URL <https://openreview.net/forum?id=2EpjkjzdCAa>.

Haoyi Zhou, Shanghang Zhang, Jieqi Peng, Shuai Zhang, Jianxin Li, Hui Xiong, and Wancai Zhang. Informer: Beyond efficient transformer for long sequence time-series forecasting. In *Thirty-Fifth AAAI Conference on Artificial Intelligence, AAAI 2021, Thirty-Third Conference on Innovative Applications of Artificial Intelligence, IAAI 2021, The Eleventh Symposium on Educational Advances in Artificial Intelligence, EAAI 2021, Virtual Event, February 2-9, 2021*, pages 11106–11115. AAAI Press, 2021a. URL <https://ojs.aaai.org/index.php/AAAI/article/view/17325>.

Haoyi Zhou, Shanghang Zhang, Jieqi Peng, Shuai Zhang, Jianxin Li, Hui Xiong, and Wancai Zhang. Informer: Beyond efficient transformer for long sequence time-series forecasting. In *The Thirty-Fifth AAAI Conference on Artificial Intelligence, AAAI 2021, Virtual Conference*, volume 35, pages 11106–11115. AAAI Press, 2021b.

Tian Zhou, PeiSong Niu, Xue Wang, Liang Sun, and Rong Jin. One fits all: power general time series analysis by pretrained lm, 2023.

A Appendix

A.1 Dataset Hosting, Licensing, and Maintenance

We share our dataset under the CC license. All of the synthetic datasets were generated from scratch by us using tailored scripts that will be shared upon publication or using available open-source repositories. We include and reformat some real-life datasets that are also shared under CC license, we appropriately cite the original work. The dataset can be accessed on the gdrive folder for the purpose of submission. Upon publication, the paper will be moved to persistent departmental storage.

A.2 Dataset Conventions

Datasets are shared as hdf5 files `dat`, which we find a convenient format to store several tensors within a single file. Each of the dataset hdf's has two keys: `train_data` and `test_data` for accessing the training trajectories and test trajectories respectively. We follow the convention of storing multiple trajectories and dimensions within a single three dimensional tensor. The first dimension corresponds to a trajectory, the second dimension to a time-stamp, and the third dimension to the state coordinate. Example `train_data` shape for the cheetah dataset reads $(18000, 1000, 17)$, i.e. there are 18k trajectories of length 1000, states are 17 dimensional. Data in the hdf files are always unnormalized, we perform data normalization during the loading process using statistics of the training data portion.

A.3 Additional Experiments

We present some additional experiments that were deferred from the main part of the paper.

A.3.1 Performance in a Scarce Training Trajectory Regime

Our benchmark datasets consist of a relatively large number of training trajectories (all synthetic datasets consists of 20k trajectories). Evaluating the NN models in a regime of scarce training trajectories is also worth investigating. We performed an experiment in which the training dataset was reduced to only 1000 trajectories and evaluated the NN models in such a scenario for a selection of datasets. We observe that in such a setting, metrics change significantly compared to the results obtained for the full datasets reported in Sec. 4. Generally, in the case of synthetic datasets presented in Tab. 6, the SpaceTime model is now stronger. Latent NLinear still outperforms its vanilla counterpart, whereas DeepAR with curriculum learning is now less performant than vanilla DeepAR. Whereas in case of the real-life datasets vanilla NLinear and N-Hits performs better, and similarly DeepAR with curriculum learning is now less performant than vanilla DeepAR. It is important to note, that NLinear and Latent NLinear here use a different algorithm, that performs a linear transformation of the lookback and adds the results to the last observation in the lookback (instead of performing the transformation on the lookback sequence that had the value last observation subtracted from each state).

A.3.2 MuJoCo D Benchmark

Results are presented in Tab. 8. Quantitatively the results are similar to those for MuJoCo S datasets, hence were omitted from the main part of the paper.

A.3.3 XGBoost experiments

We have conducted experiments that use the XGBoost [Chen and Guestrin, 2016] algorithm instead of a neural network-based model on a few datasets. The direct approach was used, which inputs the whole lookback as separate variables (flattened multivariate observations) to the model, which outputs the whole horizon at once. Other approaches yielded similar or worse test results. It is important to note that the computation time scales significantly with the lookback and history lengths, as much as the dimensionality of the states or the number of estimators used. XGBoost outperformed other tested methods on M4 and was very competitive on ETT. However, chaotic and MuJoCo datasets were underperforming on longer lookback lengths, probably due to the vast number of variables, which rendered the model unable to use them properly (e.g., Hopper dataset results in $500 \cdot 11$ input variables while having only training 18000 trajectories). The table 9 details the results. All the hyperparameters are kept constant and use their default values, apart from the max depth of the tree

Table 6: Benchmark Results on the synthetic datasets in the scarce training trajectories regime, *we limited the training sets to only 1000 trajectories and have used shorter time limits*. The resulting metrics are shown rounded to two decimal places. The numbers shown in the first table were also multiplied by 100.

DATASET	L	NLINEAR		N-HITS		LATENT NLINEAR		SPACE TIME		PATCHTST		DEEPAR CL		LSTM		DEEPAR VANILLA		NEURAL ODE	
		MSE	MAE	MSE	MAE	MSE	MAE	MSE	MAE	MSE	MAE	MSE	MAE	MSE	MAE	MSE	MAE	MSE	MAE
SIN.	8	0.0	0.0	0.0	0.0	0.0	0.0	0.0	0.4	2.0	11.1	58.0	66.1	74.2	67.7	99.2	80.6	99.5	80.8
	96	0.0	0.0	0.0	0.0	0.0	0.0	0.0	0.7	0.2	3.7	6.1	18.2	88.8	74.4	96.7	79.5	100.3	81.3
AVG.		0.0	0.0	0.0	0.0	0.0	0.0	0.0	0.6	1.1	7.4	32.0	42.1	81.5	71.1	97.9	80.0	99.9	81.1

DATASET	L	N-HITS		LATENT NLINEAR		SPACE TIME		NLINEAR		DEEPAR VANILLA		NEURAL ODE		LSTM		PATCHTST		DEEPAR CL	
		MSE	MAE	MSE	MAE	MSE	MAE	MSE	MAE	MSE	MAE	MSE	MAE	MSE	MAE	MSE	MAE	MSE	MAE
M.-G.	96	0.74	0.62	0.77	0.64	0.76	0.66	0.83	0.71	0.99	0.81	0.98	0.81	0.99	0.82	0.84	0.69	0.93	0.78
	500	0.88	0.73	0.92	0.76	0.83	0.72	0.94	0.78	0.97	0.81	0.96	0.80	0.96	0.80	1.01	0.81	0.99	0.81
	1000	0.91	0.76	0.96	0.79	0.99	0.82	1.02	0.81	0.96	0.80	0.97	0.80	0.96	0.80	1.06	0.84	0.97	0.80
L.-V.	96	0.88	0.66	0.89	0.66	0.87	0.67	0.90	0.69	1.00	0.75	0.99	0.71	0.95	0.73	1.08	0.74	1.00	0.74
	500	0.84	0.63	0.87	0.64	0.83	0.65	0.88	0.66	0.86	0.65	0.98	0.73	0.95	0.72	1.06	0.72	1.53	0.84
	1000	0.80	0.60	0.91	0.66	1.05	0.77	0.95	0.70	0.98	0.70	0.94	0.68	1.00	0.73	1.16	0.77	1.43	0.79
AVG.		0.84	0.67	0.89	0.69	0.89	0.72	0.92	0.72	0.96	0.75	0.97	0.76	0.97	0.77	1.03	0.76	1.14	0.79

DATASET	L	LSTM		SPACE TIME		LATENT NLINEAR		DEEPAR VANILLA		DEEPAR CL		N-HITS		NEURAL ODE		NLINEAR		PATCHTST	
		MSE	MAE	MSE	MAE	MSE	MAE	MSE	MAE	MSE	MAE	MSE	MAE	MSE	MAE	MSE	MAE	MSE	MAE
CHEETAH S	96	0.82	0.73	0.83	0.74	0.83	0.74	0.94	0.82	0.95	0.82	0.93	0.78	0.96	0.83	0.95	0.78	0.99	0.81
	250	0.79	0.71	0.81	0.73	0.81	0.73	0.94	0.82	0.94	0.76	0.99	0.80	0.96	0.83	1.06	0.82	1.00	0.81
	500	0.71	0.66	0.74	0.68	0.76	0.70	0.94	0.82	0.81	0.68	0.97	0.78	0.96	0.83	1.10	0.82	0.95	0.78
HOPPER D	96	0.60	0.43	0.60	0.44	0.62	0.44	0.63	0.45	0.66	0.48	0.60	0.44	0.75	0.53	0.63	0.46	1.18	0.61
	250	0.65	0.46	0.67	0.48	0.69	0.50	0.70	0.49	0.80	0.56	0.69	0.50	0.77	0.54	0.74	0.54	1.28	0.68
	500	0.57	0.43	0.58	0.45	0.64	0.48	0.65	0.49	0.68	0.49	0.65	0.50	0.70	0.49	0.84	0.59	1.11	0.67
AVG.		0.69	0.57	0.70	0.59	0.73	0.60	0.80	0.65	0.81	0.63	0.81	0.63	0.85	0.67	0.89	0.67	1.08	0.73

Table 7: Benchmark Results on the real-life datasets in the scarce training trajectories regime, *we limited the training sets to only 1000 trajectories and have used shorter time limits*. The resulting metrics are shown rounded to two decimal places.

DATASET	L	N-HITS		NLINEAR		LATENT NLINEAR		SPACE TIME		LSTM		PATCHTST		DEEPAR VANILLA		DEEPAR CL		NEURAL ODE	
		MSE	MAE	MSE	MAE	MSE	MAE	MSE	MAE	MSE	MAE	MSE	MAE	MSE	MAE	MSE	MAE	MSE	MAE
ETTM1+2	720	0.17	0.30	0.16	0.29	0.16	0.29	0.32	0.42	0.19	0.32	0.23	0.36	0.39	0.50	0.31	0.42	0.49	0.58
	336	0.19	0.32	0.19	0.32	0.19	0.32	0.19	0.32	0.22	0.34	0.26	0.37	0.34	0.44	0.44	0.47	1.50	0.93
	96	0.22	0.34	0.23	0.34	0.22	0.33	0.22	0.34	0.25	0.36	0.32	0.41	0.53	0.54	0.73	0.71	0.51	0.55
ETTM (LONG)	1000	0.19	0.32	0.18	0.31	0.16	0.29	0.21	0.34	0.18	0.31	0.25	0.37	0.32	0.43	0.36	0.45	NAN	NAN
M4	168	0.14	0.17	0.16	0.19	0.15	0.18	0.18	0.20	0.15	0.19	0.30	0.28	0.17	0.22	0.16	0.20	0.16	0.19
	96	0.24	0.24	0.26	0.25	0.25	0.25	0.26	0.27	0.25	0.26	0.30	0.28	0.37	0.34	0.30	0.29	0.25	0.25
AVG.		0.15	0.23	0.16	0.23	0.16	0.23	0.18	0.25	0.19	0.25	0.26	0.29	0.29	0.34	0.33	0.35	0.45	0.40

DATASET	L	LSTM		LATENT NLINEAR		SPACE TIME		DEEPAR VANILLA		DEEPAR CL		PATCHTST	
		MSE	MAE	MSE	MAE	MSE	MAE	MSE	MAE	MSE	MAE	MSE	MAE
PEMS_BAY	144	0.64	0.36	0.68	0.40	0.68	0.39	0.72	0.38	0.74	0.38	0.87	0.45

that is set to 3, the regression objective is the squared error, the tree method is set to ‘gpu_hist’ and the number of estimators is varied and shown in Tab. 9.

Table 8: Benchmark Results on the MuJoCo D datasets described in Sec. 2.1.

DATASET	L	DEEPAR CL		LSTM		LATENT NLINEAR		SPACE TIME		N-HITS		NLINEAR		DEEPAR VANILLA		NEURAL ODE	
		MSE	MAE	MSE	MAE	MSE	MAE	MSE	MAE	MSE	MAE	MSE	MAE	MSE	MAE	MSE	MAE
CHEETAH(D)	96	0.78	0.71	0.79	0.71	0.80	0.72	0.79	0.71	0.81	0.72	0.81	0.72	0.92	0.79	0.93	0.81
	250	0.75	0.68	0.76	0.69	0.77	0.70	0.77	0.70	0.80	0.71	0.79	0.71	0.96	0.83	0.95	0.82
	500	0.65	0.62	0.66	0.63	0.69	0.64	0.68	0.64	0.75	0.68	0.72	0.66	0.94	0.82	0.91	0.80
HOPPER(D)	96	0.58	0.42	0.56	0.41	0.58	0.42	0.59	0.43	0.56	0.41	0.61	0.43	0.58	0.42	0.63	0.47
	250	0.60	0.44	0.60	0.44	0.61	0.45	0.64	0.47	0.62	0.46	0.66	0.48	0.60	0.44	0.66	0.48
	500	0.44	0.38	0.43	0.37	0.49	0.42	0.50	0.42	0.51	0.43	0.56	0.46	0.45	0.39	0.54	0.45
WALKER(D)	96	0.73	0.53	0.73	0.52	0.74	0.53	0.74	0.53	0.74	0.53	0.74	0.53	0.74	0.53	0.75	0.55
	250	0.83	0.59	0.83	0.59	0.84	0.60	0.84	0.60	0.85	0.61	0.86	0.61	0.83	0.59	0.85	0.61
	500	0.79	0.55	0.80	0.56	0.89	0.62	0.87	0.62	0.93	0.64	0.96	0.67	0.82	0.56	0.86	0.60
AVG.		0.68	0.55	0.69	0.55	0.71	0.57	0.71	0.57	0.73	0.58	0.74	0.59	0.76	0.60	0.79	0.62

Table 9: Summary of test MSE for different lookback lengths and datasets using XGBoost estimator

L	DATASET	MSE	# OF ESTIMATORS
96	ETTM1+2	0.220	32
336	ETTM1+2	0.176	32
720	ETTM1+2	0.148	32
96	M4	0.167	32
168	M4	0.097	32
96	M.-G.	0.724	32
500	M.-G.	0.806	32
1000	M.-G.	0.811	32
96	M.-G.	0.714	16
250	M.-G.	0.747	16
500	M.-G.	0.710	16

A.4 Parameter Counts

In the paper, we benchmarked representatives of diverse NN model classes whose parameter efficiency varies significantly. We summarize in Tab. 10 the parameter counts of all of the tested models providing insights on how the NN models scale with respect to the state dimension and encoded sequence length.

A.5 Open-source Software Description

Our software library shared online cod includes custom implementations of DeepAR, LSTM, LatentODE, NLinear, and Latent NLinear models. We modified the original N-Hits (which we could not distribute due to licensing issues) and SpaceTime implementations to fit our workflows, including support for multivariate series in the N-Hits model. Our framework offers full training and validation workflows, with monitoring and visualizations via ML-Ops (we used neptune.ai). It is designed to be modular, allowing users to swap datasets, trainer configurations, and models easily. We will release the code on GitHub under Apache 2.0 license upon publishing the paper. Instructions are available in the README file within the zipped software package.

A.6 Hyperparameters

In Tab. 11 we present hyperparameters for the main dataset classes representatives.

We have tuned the most important hyperparameters of the two introduced models (Latent NLinear & DeepAR + CL). In the case of Latent NLinear, we varied the encoder width and the latent space dimension. We find that the latent NLinear model is pretty robust w.r.t. its hyperparameters. In the case of DeepAR + CL, we varied the model depth and the hidden dimension. The results for DeepAR + CL are generally within the std.dev. margin for the smaller architectures and deteriorate when using larger architectures (hidden dim > 128 or depth > 3). We provide a simple ablation study in Tab. 12.

Table 10: Parameter counts for the benchmarked NN models. The parameter count numbers are rounded down and provided in thousands.

DATASET	MODEL	ENC. LEN.	PARAM. COUNT	ENC. LEN.	PARAM. COUNT	ENC. LEN.	PARAM. COUNT
CHEETAH	LATENT ODE	96	190k	250	190k	500	190k
CHEETAH	NLINEAR	96	25095k	250	54200k	500	72258k
CHEETAH	LATENT NLINEAR	96	34897k	250	75181k	500	100176k
CHEETAH	DEEPAR	96	341k	250	341k	500	341k
CHEETAH	LSTM	96	420k	250	420k	500	420k
CHEETAH	SPACE TIME	96	57k	250	57k	500	57k
CHEETAH	N-HITS	96	195641k	250	254696k	500	350382k
CHEETAH	PATCHTST	96	4913k	250	4921k	500	4934k
LORENZ	LATENT ODE	96	177k	500	177k	1000	177k
LORENZ	NLINEAR	96	1650k	500	6754k	1000	9003k
LORENZ	LATENT NLINEAR	96	18454k	500	75172k	1000	100167k
LORENZ	DEEPAR	96	203k	500	203k	1000	203k
LORENZ	LSTM	96	407k	500	407k	1000	407k
LORENZ	SPACE TIME	96	53k	500	53k	1000	53k
LORENZ	N-HITS	96	9738k	500	14563k	1000	20537k
LORENZ	PATCHTST	96	4769k	500	4790k	1000	4816k
K.-S.	LATENT NLINEAR	96	8883k	250	18953k	500	25201k
K.-S.	DEEPAR	96	394k	250	394k	500	394k
K.-S.	LSTM	96	776k	250	776k	500	776k
K.-S.	SPACE TIME	96	78k	250	78k	500	78k
K.-S.	PATCHTST	96	209817k	250	240505k	500	160192k
ETDATASET	LATENT ODE	96	367k	336	367k	720	367k
ETDATASET	NLINEAR	96	130k	336	372k	720	519k
ETDATASET	LATENT NLINEAR	96	654k	336	1622k	720	2211k
ETDATASET	DEEPAR	96	331k	336	331k	720	331k
ETDATASET	LSTM	96	662k	336	662k	720	662k
ETDATASET	SPACE TIME	96	72k	336	72k	720	72k
ETDATASET	N-HITS	96	861k	336	1180k	720	1692k
ETDATASET	PATCHTST	96	10938k	336	23410k	720	31319k
PEMS-BAY	LATENT NLINEAR	144	343537k				
PEMS-BAY	DEEPAR	144	1733k				
PEMS-BAY	LSTM	144	3382k				
PEMS-BAY	SPACE TIME	144	454k				
PEMS-BAY	PATCHTST	144	212608k				

Table 11: Table listing the hyperparameters of all of the studied models.

dataset	model	hyperparameters
Cheetah	latent ODE	enc: LSTM (2 layers, 50 hidden dim, 18 - out dim), ode: MLP (3 x 100-dim hidden, ELU act.), dec: MLP (4 x 200-dim hidden, ELU act.)
Cheetah	NLinear	Linear(Lookback x Horizon)
Cheetah	latent NLinear	enc: LSTM (2 layers, 50 hidden dim, 20 - out dim), Linear((Lookback · 20) x (Horizon · 20)), dec: MLP (4 x 200-dim hidden, ELU act.)
Cheetah	DeepAR	Enc and Prob. model (the same): LSTM(3 layers, 128 hidden dim), dec: Linear(128, obs. dim)
Cheetah	LSTM	Enc: LSTM(3 layers, 100 hidden dim), rnn: LSTM(3 layers, 100 hidden dim), dec: Linear(100, obs. dim)
Cheetah	SpaceTime	mostly default from the original repo, see the code for the details
Cheetah	N-Hits	shared weights=False, batchnorm=False, ReLU act., 3 stacks, 9 blocks, 2 layers in block, 128 hidden dim, pool kernel size=2, [168, 24, 1] downsample freqs, linear interpolation, dropout=0, max pooling
Cheetah	PatchTST	3 layers, 512 hidden dim, 16 heads, dropout = 0.2, patch len = 10, stride = 10
Lorenz	latent ODE	enc: LSTM (2 layers, 50 hidden dim, 4 - out dim), ode: MLP (3 x 100-dim hidden, ELU act.), dec: MLP (4 x 200-dim hidden, ELU act.)
Lorenz	NLinear	Linear((Lookback · obs. dim) x (Horizon · obs. dim))
Lorenz	latent NLinear	enc: LSTM (2 layers, 50 hidden dim, 10 - out dim), Linear((Lookback · 10) x (Horizon · 10)), dec: MLP (4 x 200-dim hidden, ELU act.)
Lorenz	DeepAR	Enc and Prob. model (the same): LSTM(3 layers, 100 hidden dim), dec: Linear(100, obs. dim)
Lorenz	LSTM	Enc: LSTM(3 layers, 100 hidden dim), rnn: LSTM(3 layers, 100 hidden dim), dec: Linear(100, obs. dim)
Lorenz	SpaceTime	mostly default from the original repo, see the code for the details
Lorenz	N-Hits	shared weights=False, batchnorm=False, ReLU act., 3 stacks, 9 blocks, 2 layers in block, 128 hidden dim, pool kernel size=2, [168, 24, 1] downsample freqs, linear interpolation, dropout=0, max pooling
Lorenz	PatchTST	3 layers, 512 hidden dim, 16 heads, dropout = 0.2, patch len = 10, stride = 10
K.-S.	latent NLinear	enc: LSTM (2 layers, 50 hidden dim, 40 - out dim), Linear((Lookback · 40) x (Horizon · 40)), dec: MLP (4 x 200-dim hidden, ELU act.)
K.-S.	DeepAR	Enc and Prob. model (the same): LSTM(3 layers, 128 hidden dim), dec: Linear(128, obs. dim)
K.-S.	LSTM	Enc: LSTM(3 layers, 128 hidden dim), rnn: LSTM(3 layers, 128 hidden dim), dec: Linear(128, obs. dim)
K.-S.	SpaceTime	mostly default from the original repo, see the code for the details
K.-S.	PatchTST	3 layers, 256/128/64 hidden dim, 16 heads, dropout = 0.2, patch len = 10, stride = 10
ETDataset	latent ODE	enc: LSTM (2 layers, 128 hidden dim, 16 - out dim), ode: MLP (3 x 128-dim hidden, ELU act.), dec: MLP (4 x 200-dim hidden, ELU act.)
ETDataset	NLinear	Linear(Lookback x Horizon)
ETDataset	latent NLinear	enc: LSTM (2 layers, 32 hidden dim, 2 - out dim), Linear((Lookback · 2) x (Horizon · 2)), dec: MLP (4 x 200-dim hidden, ELU act.)
ETDataset	DeepAR	Enc and Prob. model (the same): LSTM(3 layers, 64 hidden dim), dec: Linear(64, obs. dim)
ETDataset	LSTM	Enc: LSTM(3 layers, 128 hidden dim), rnn: LSTM(3 layers, 128 hidden dim), dec: Linear(128, obs. dim)
ETDataset	SpaceTime	mostly default from the original repo, see the code for the details
ETDataset	N-Hits	shared weights=False, batchnorm=False, ReLU act., 3 stacks, 9 blocks, 2 layers in block, 128 hidden dim, pool kernel size=2, [168, 24, 1] downsample freqs, linear interpolation, dropout=0, max pooling
ETDataset	PatchTST	3 layers, 512 hidden dim, 16 heads, dropout = 0.2, patch len = 10, stride = 10
Pems-Bay	latent NLinear	enc: LSTM (2 layers, 256 hidden dim, 128 - out dim), Linear((Lookback · 128) x (Horizon · 128)), dec: MLP (4 x 200-dim hidden, ELU act.)
Pems-Bay	DeepAR	Enc and Prob. model (the same): LSTM(3 layers, 256 hidden dim), dec: Linear(256, obs. dim)
Pems-Bay	LSTM	Enc: LSTM(3 layers, 256 hidden dim), rnn: LSTM(3 layers, 256 hidden dim), dec: Linear(256, obs. dim)
Pems-Bay	SpaceTime	mostly default from the original repo, see the code for the details
Pems-Bay	PatchTST	3 layers, 320 hidden dim, 16 heads, dropout = 0.2, patch len = 10, stride = 10

Table 12: Table listing the hyperparameters that we tuned for the introduced methods (Latent NLinear and DeepAR + CL)

method	dataset	hyperparameters	MSE	MAE
Latent NLinear	ETT	latent dim=2, hidden dim=16	0.152	0.287
Latent NLinear	ETT	latent dim=2, hidden dim=32	0.152	0.286
Latent NLinear	ETT	latent dim=2, hidden dim=64	0.151	0.286
Latent NLinear	ETT	latent dim=2, hidden dim=128	0.151	0.285
Latent NLinear	ETT	latent dim=4, hidden dim=128	0.151	0.287
Latent NLinear	ETT	latent dim=8, hidden dim=128	0.154	0.288
Latent NLinear	ETT	latent dim=16, hidden dim=128	0.152	0.289
DeepAR + CL	ETT	hidden dim=32, depth=3	0.177	0.308
DeepAR + CL	ETT	hidden dim=64, depth=3	0.174	0.310
DeepAR + CL	ETT	hidden dim=128, depth=3	0.174	0.308
DeepAR + CL	ETT	hidden dim=256, depth=3	0.411	0.487
DeepAR + CL	ETT	hidden dim=128, depth=4	0.263	0.365
DeepAR + CL	ETT	hidden dim=128, depth=2	0.150	0.290